A Wideband Dual-Cavity-Backed Polarization Reconfigurable Antenna Based on Liquid Metal Switches

Yuwei Zhang[1], Shu Lin[2], Libo Wang[2], and Qun Ding[1, *]

Abstract—This letter presents a wideband polarization reconfigurable antenna based on liquid metal (LM) switches. It consists of single-fed crossed bowtie dipoles, a parasitic element grounded via a metallic post, a dual-cavity-backed reflector, and liquid metal switches. The two arms of one dipole are loaded with two symmetrical identical slots, and on top of the slots, two sets of fixed-length movable liquid metal columns filled in polytetrafluoroethylene (PTFE) tubes are attached as switches. The altering between linear polarization (LP) and circular polarization (CP) can be achieved by changing the positions of the liquid metal switches. The dual-cavity structure is applied to obtain unidirectional radiation and enhance the circularly polarized performance. A prototype with overall size of $127 \times 127 \times 57\,\text{mm}^3$ is designed and fabricated. The measured results indicate that the impedance bandwidth (IBW) of the antenna is from 1.06 to 2.46 GHz (79.54%), and the axial ratio bandwidth (ARBW) is from 1.39 to 1.91 GHz (31.52%) for CP state. In addition, the IBW for LP state is from 1.06 to 2.30 GHz (73.81%). Moreover, the peak gains can reach 7.73 dBic in CP state and 9.21 dBi in LP state.

1. INTRODUCTION

Nowadays, polarization reconfigurable antennas have received extensive attention because of their ability to reduce polarization mismatch and increase channel capacity and quality. The most common approaches to achieve reconfigurability are currently using tunable elements such as PIN diodes [1], variable capacitors [2], microelectromechanical systems (MEMSs) switches [3], but in contrast, LM-based reconfiguration is a promising technique because LM-Galinstan has low loss, non-toxicity, and easy control [4]. In recent years, many studies have used liquid metals to achieve reconfigurability, especially frequency and pattern reconfigurations [4–8], while the researches to achieve polarization reconfiguration are mostly for inter-linear polarization [9–11]. In [12], an aperture-coupled patch antenna composed of liquid metal alloy and copper tape is proposed, and the polarization reconfiguration (between LP and CP) is achieved by changing the position of the liquid metal in four triangle cavities. The overlapping operation band determined by the CP bandwidth of the antenna is 3.06%. Paper [13] presents a slot antenna, and by filling the microchannels with liquid metal, the LP, left-hand circular polarization (LHCP), and right-hand circular polarization (RHCP) can be all obtained. The 3-dB ARBW is 26.42% for the CP states, but the IBW is only 11.6% in LP state. In [14], multipolarization reconfiguration is achieved by an E-shaped patch antenna with liquid metal tunable slots, and the working bandwidths are still narrow for all states.

In this letter, a liquid metal (LM) based polarization reconfigurable antenna is proposed. This antenna is a design based on a self-phased circularly polarized crossed bowtie dipole antenna. The main radiators of the antenna are two orthogonal bowtie dipoles with the same contour. Two symmetric

* Corresponding author: Qun Ding (qunding@aliyun.com).
[1] School of Electronics Engineering, Heilongjiang University, Harbin, China. [2] School of Electronics and Information Engineering, Harbin Institute of Technology, Harbin, China.

slots are etched on one dipole to realize CP radiation. In addition, two sets of LM columns filled in the PTFE tubes are loaded on the surface of the dipole's arms. By using air pressure, the position of the LM columns can be changed. Since the LMs are coupled with the radiators, placing them above the slots or moving them away can make the slots open or short, at which time the LM columns achieve the role of switches. By controlling the LM switches, the phase changes between the dipoles can be realized, and the switching between LP and CP can be realized. The use of the bowtie dipoles, the parasitic element, and the dual-cavity backed reflector can improve the IBW and ARBW of the antenna effectively.

2. ANTENNA DESIGN AND ANALYSIS

2.1. Antenna Configuration

Figure 1 shows the geometry of the proposed antenna. It consists of single-fed crossed bowtie dipoles, a parasitic bowtie patch grounded via a metallic post, a dual-cavity-backed reflector, and liquid metal switches. The dipoles and parasitic element are printed on an FR4 substrate ($\varepsilon_r = 4.4$, $\tan\delta = 0.005$) with a dimension of $130 \times 130 \times 1\,\text{mm}^3$ and excited by a $50\,\Omega$ coaxial cable. The coaxial cable is connected to the dipoles' arms through an RF coaxial connector SMA-KE which is intercepted two pins. Two symmetrical slots which are served as capacitive loadings are etched on one dipole to generate CP mode. A dual-cavity-backed reflector is employed to achieve unidirectional radiation and wide ARBW, which provide two radiating apertures. The aperture' size and height of the cavity are W_n^2 and H_n^2 ($n = 1$ or 2), and $H_1 + H_2$ is equal to $0.25\lambda_0$ (λ_0 is the wavelength at $1.31\,\text{GHz}$ which is the lowest CP operating frequency). Two sets of (six) fixed-length LM columns filled in the PTFE tubes are loaded on the surface of the dipole's arms. To prevent the LM surfaces from sticking to the tubes' walls due
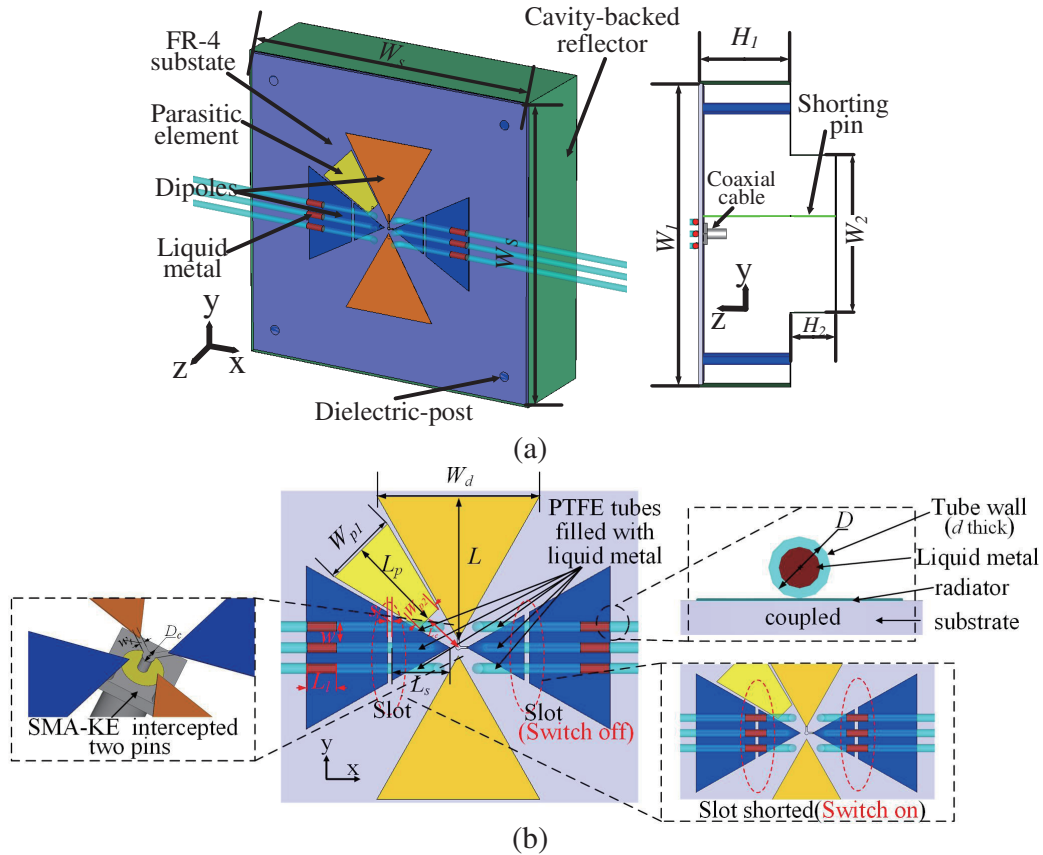
Figure 1. Geometry of the proposed antenna. (a) 3D and side views. (b) Front view of the radiator.

to oxidation, NaOH is added in the tubes. Air pumps are used at the ends of the tubes to generate air pressures to push the LM columns. When the LM columns are moved to the positions over the slots, the arms of the slots are shorted because of the coupled connection between the LMs and the arms. At this time, the two dipoles are fed by the same coaxial line, and the currents' amplitudes and phases at the feed point of the two dipoles are equal, so the antenna works in the LP mode. While the LM columns move away from the slots, the arms of the slots are opened. Loading these slots changes the phase of one dipole, and the phase difference between the two dipoles is approximately $90°$, so the antenna operates in CP state. As seen, the LM columns can be used as RF switches. By controlling the switches, the polarization reconfiguration can be realized. The optimum dimensions of the proposed antenna are listed in Table 1.

Table 1. Geometric parameters for the proposed antenna (unit: mm).

| Parameter	Value	Parameter	Value	Parameter	Value	Parameter	Value	Parameter	Value
W_s	127	W_1	125	W_2	66	W_{p1}	18	W_{p2}	6.5
W_d	39.2	w_t	0.5	w	5	H_1	38	H_2	19
L_l	7	L_s	13.8	L_c	10	L_p	23	L	34.5
s	1.2	D_c	1.19	D	2.7	d	0.2		

2.2. Liquid Metal Switches

In this paper, LM column with mobility is used to design the switch structure in the radiator of antenna as a way to obtain reconfiguration. Here the feasibility of using LM column as an RF switch will be discussed. A section of microstrip line with an impedance of $50\,\Omega$ and a slot of $1\,\text{mm}$ width is given in Fig. 2. An LM column ($2\,\text{mm}$ in diameter) loaded in a PTFE tube ($\varepsilon_r = 2.8$ and $\tan\delta = 0.0005$) is placed above the slot of the microstrip line, and the distance between the LM column and the metal strip (i.e., the thickness of the tube's wall) is d. At this time, the LM column is equivalent to a switch structure, and the slot can be opened (at switch "off") or shorted (at switch "on") by the coupling action. The $|S_{11}|$ and $|S_{21}|$ curves of this structure when the switch is turned on are given in Fig. 3 (a). It can be seen that as the wall's thickness d increases, the transmission capability decreases. Meanwhile, the transmission bandwidth also decreases. However, the total transmission can be achieved even at $5.16\,\text{GHz}$. On the other hand, the reflection coefficient $|S_{11}|$ is also minimized at $5.16\,\text{GHz}$, and the impedance bandwidth becomes smaller as the value of d increases.

The above results illustrate that the use of LM column as a switch can achieve the shorting of the slot, but the increase in d causes a reduction in the coupling between the LM and the metal strip, which affects the bandwidth characteristic. When moving the LM column away from the slot, the switch is
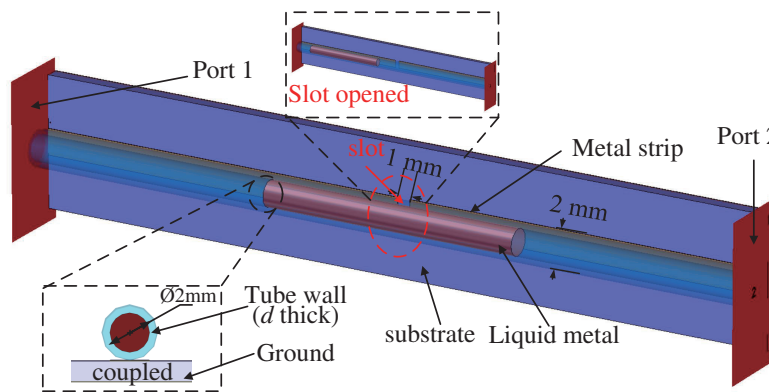
**Figure 2.** Geometry of the microstrip structure with LM switch.
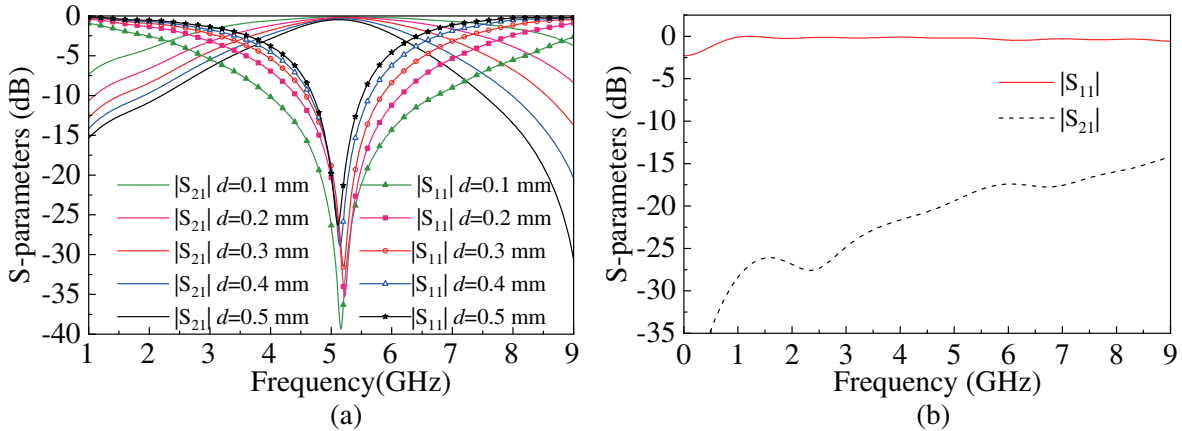
Figure 3. *S*-parameters of the structure (a) at switch "on" state. (b) at switch "off" state.

at the "off" state. Fig. 3(b) gives the *S*-parameters of the microstrip line ($d = 0.5$ mm) at switch "off" state. It is obvious that the values of $|S_{11}|$ almost all converge to 0 dB, and the values of $|S_{21}|$ are all less than -15 dB, which achieves total reflection. Therefore, the slot is opened. It is confirmed that a movable LM column can be employed as a switch within a certain frequency band.

2.3. Working Mechanism

To clearly illustrate the working mechanism, the design procedure of the antenna is demonstrated in Fig. 4(a). The corresponding voltage standing wave ratios (VSWRs) and axial ratios (ARs) are shown in Figs. 4(b) and (c). There are four steps of the antenna design. In step 1, the antenna is composed of the two crossed bowtie dipoles which are fed by the same coaxial cable. The antenna works in the LP state. As shown in Figs. 4(b) and (c), the values of the ARs are all 40 dB, and the IBW with VSWR < 2 is from 1.47 to 2.22 GHz. In step 2, when the capacitive slots are inserted into the horizontal dipole, this dipole becomes the phase leading component, so the phase difference between the two dipoles is changed. The right handed CP (RHCP) performance is achieved. In this step, the 3-dB ARBWs are 15.27% from 1.33 to 1.55 GHz and 5.87% from 1.83 to 1.93. The IBWs are 9.43% from 1.01 to 1.11 GHz
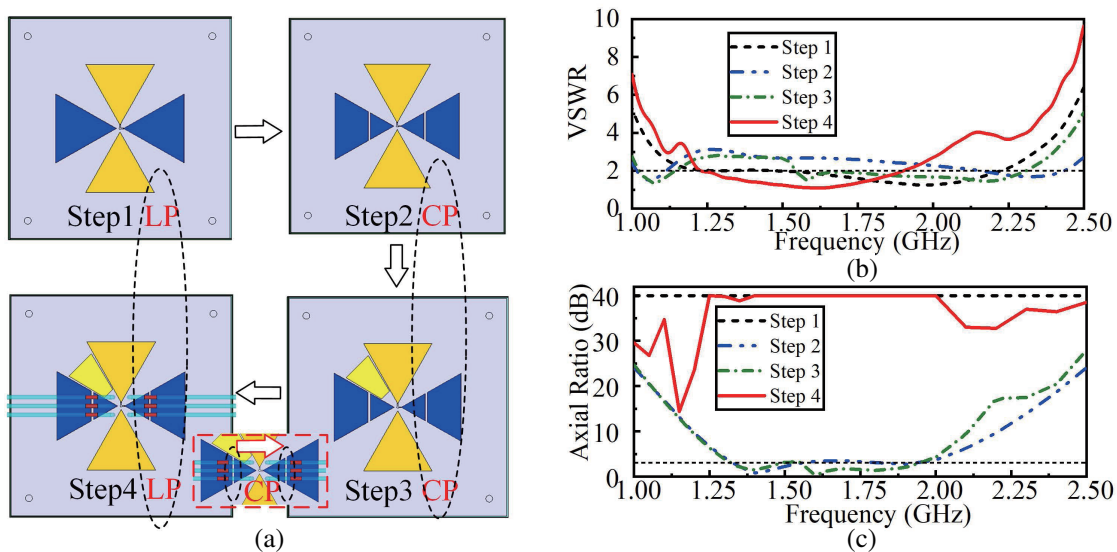
Figure 4. (a) Design procedure of the proposed antenna with four step. (b) Simulated VSWRs of four antennas. (c) Simulated ARs of four antennas.

and 12.27% from 2.15 to 2.43. In step 3, to improve the IBW and ARBW, a trapezoid parasitic element shorted to the ground is loaded at the gap between two dipole's arms. The IBW is extended to 40% (1.54–2.31 GHz) and the ARBW is increased to 39.26% (1.31–1.95 GHz). At this time, the designed antenna is changed from a linearly polarized antenna to a circularly polarized antenna with a wide operation bandwidth. In step 4, in order to achieve the switching between LP and CP, the LM switches are loaded on the top of the slots. By controlling the switches, the slots can be opened and shorted. As shown in Fig. 4, when the switches are turned on, the ARs of the antenna are approximately 40 dB at 1.25–2.1 GHz, and the antenna changes to LP working state. The IBW is 42.8% from 1.23 to 1.90 GHz. When the switches are turned off (moving the LMs away from the slots), the antenna turns back to CP mode. Finally, the antenna achieves wideband polarization reconfiguration characteristic. Usually, the antenna uses a metal plate as a reflector to achieve directional radiation characteristic. In this paper, a dual-cavity reflector is employed to obtain better antenna performance. Compared with using a flat plate as a reflector, using a cavity structure with four rims is equivalent to introducing a new radiation structure, so it can effectively improve the radiation characteristics of the antenna [15]. In addition, using a dual-cavity structure is equivalent to bringing two new radiation structures, and the antenna performance can be further improved. Taking the CP state as an example, Fig. 5 gives the gains and ARs of the antenna when loading a metal plate, a single cavity or a dual-cavity at the same distance from the radiator of the antenna, respectively. It can be clearly seen that loading single cavity can improve the antenna's gains and ARs, and when the single cavity is evolved into dual cavities, the antenna performance is improved again, and higher gains and wider ARBW are obtained.
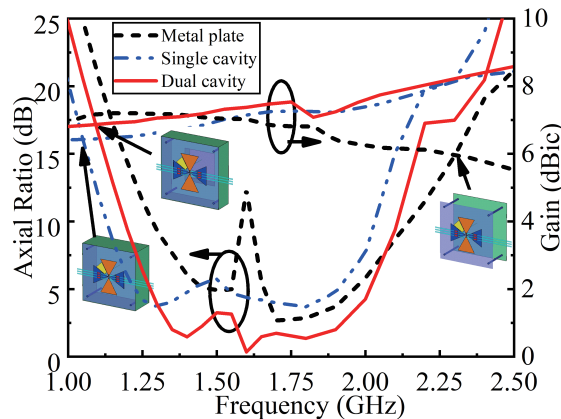
Figure 5. Comparison of the gains and ARs of the antenna in CP state when it is loaded with the single or dual cavity reflector and with the metal plate.

3. RESULT AND DISCUSSION

A prototype of the proposed antenna, as shown in Fig. 6, was fabricated and measured. The LM columns are injected into six PTFE tubes and controlled by the air pressures. This antenna has two working states. When the LM switches are turned on, the antenna works in the LP state. When the LM switches are turned off, the antenna works in the RHCP state. This proposed antenna has been measured in an anechoic chamber by the Agilent N5227A vector network analyzer. Fig. 7 shows the measured and simulated VSWRs of the two states. The measured IBWs for VSWR < 2 of 73.81% from 1.06 GHz to 2.3 GHz and of 79.55 % from 1.06 GHz to 2.46 GHz are obtained at LP and CP states, respectively. Fig. 8 gives the simulated and measured ARs at CP state and gains/efficiencies at the two states. As can be seen, the measured 3 dB ARBW of 1.39–1.91 GHz is achieved, and the efficiencies are all higher than −1.02 dB (79%) in the overlapping operating band determined by the 3 dB ARBWs. Moreover, the measured peak gains are 9.21 dBi and 7.73 dBic for the two states. Fig. 9 displays the simulated and measured radiation patterns of the proposed antenna. As seen, the antenna has good directional radiation characteristic in the operation band. A good agreement between the simulated and measured
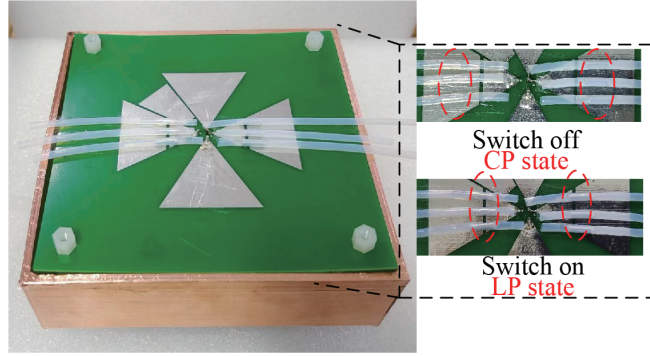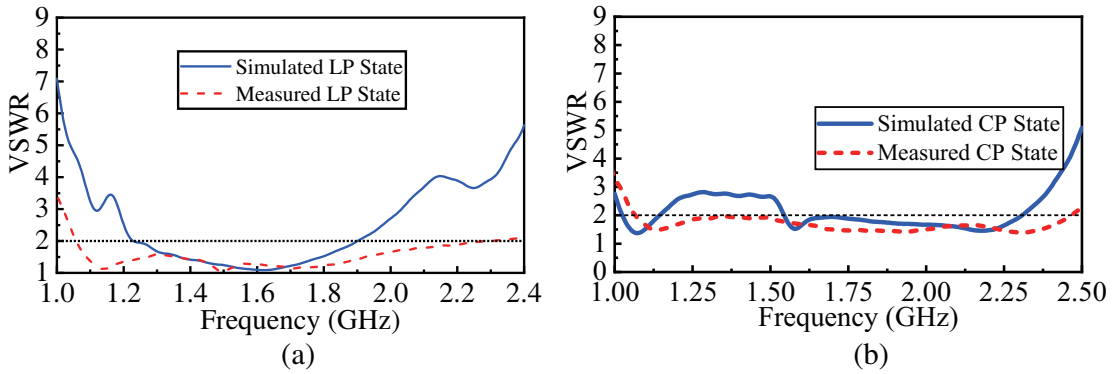
Figure 6. Prototype of the proposed antenna.

(a)   (b)

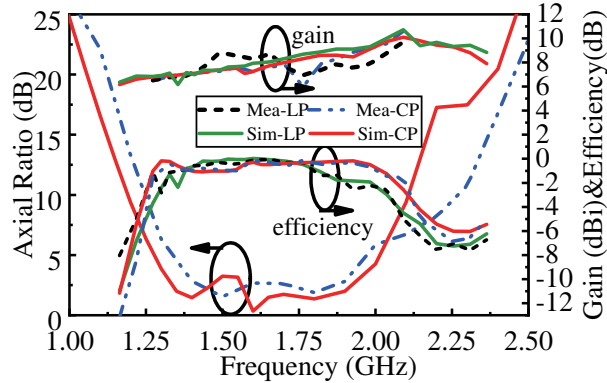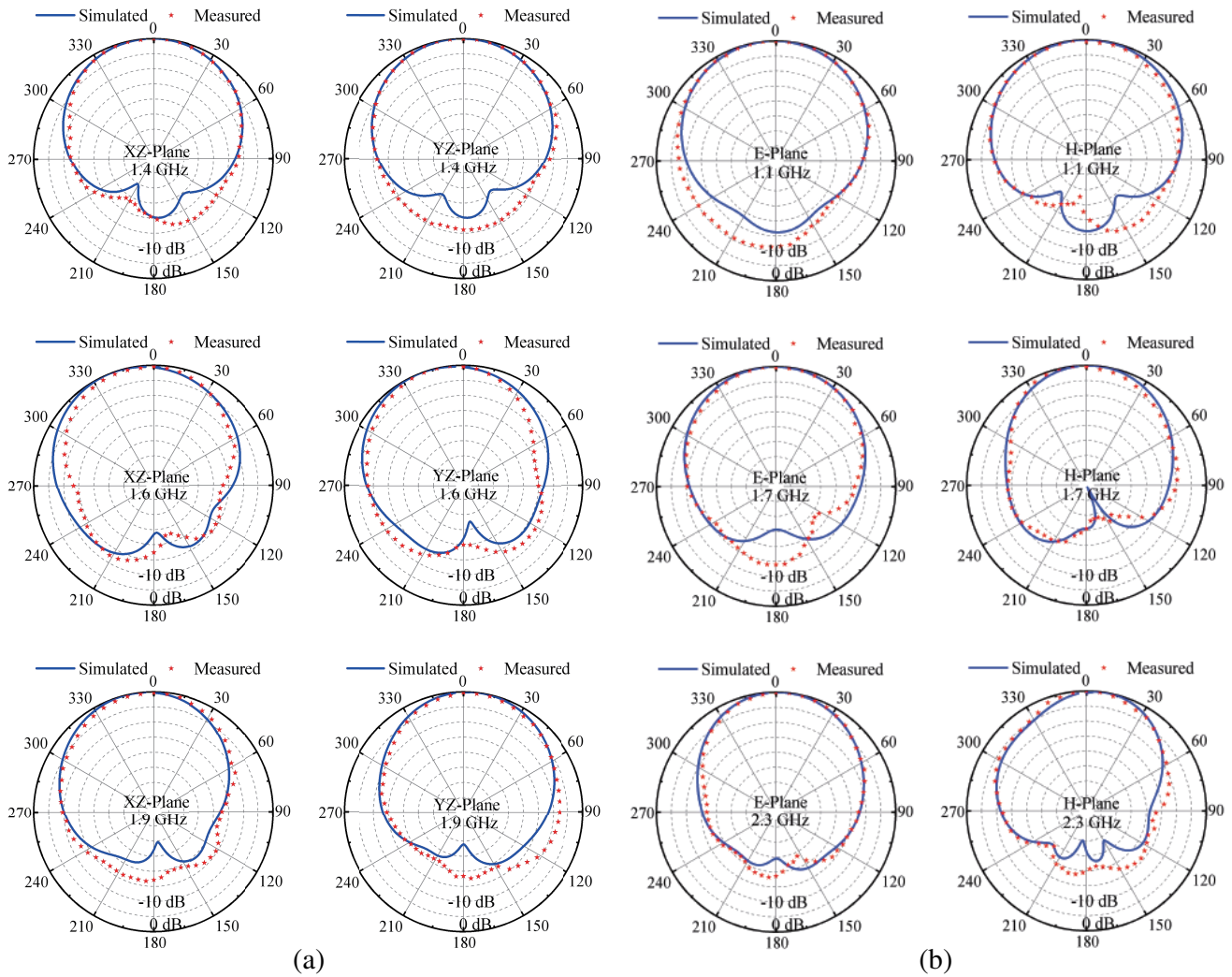**Figure 7.** Simulated and measured VSWRs of the proposed antenna.(a) LP state. (b) CP state.

Figure 8. Simulated and measured ARs, gains and efficiencies of the proposed antenna.

results is observed, and the tiny discrepancy between them might be due to the fabrication errors. Moreover, the differences between simulation and measurement are also caused by the interference from the tool used to fix the antenna for measurement.

Table 2 shows the comparison between the proposed antenna and other antennas. All these antennas are linear and circular polarization reconfigurable antennas based on liquid metal, and they have different radiator types. As seen, the proposed antenna has the highest peak gain and best bandwidth performance.

Figure 9. Simulated and Measured normalized radiation patterns of the proposed antenna (a) for CP state. (b) for LP state.

Table 2. Comparison between the proposed antenna and other antennas.

Ref.	Peak Gain	IBW in LP	IBW in CP	ARBW in CP	Radiator Type
[12]	7.33 dBic	23.2%	36.3%	3.6%	Aperture-coupled Patch
[13]	3.97 dBic	11.6%	37%	11.24%	Slot
[14]	8.1 dBi	10.4% (−8 dB)	10% (−8 dB)	Not Mentioned	E-Shaped Patch
Proposed Antenna	9.21 dBi	73.81%	79.55%	31.52%	Crossed Bowtie Dipoles

4. CONCLUSION

A dual-cavity-backed antenna using liquid metal columns as switches for polarization reconfiguration is investigated. Based on single-fed crossed dipoles antenna, two slots are etched on one dipole's arms. The slots can be shorted and opened by controlling the LM switches. Accordingly, the phase difference between the two dipoles is changed, and the polarization reconfiguration can be obtained. In addition, using the dual-cavity structure can improve the antenna's performance effectively. The measured results show that the antenna achieves wide IBWs for both the CP and LP states and also obtains a wide ARBW for the CP state. The peak gain of the proposed antenna can reach 9.21 dBi.

ACKNOWLEDGMENT

REFERENCES

1. Ye, Q. C., J. L. Li, and Y. M. Zhang, "A circular polarization-reconfigurable antenna with enhanced axial ratio bandwidth," *IEEE Antennas and Wireless Propagation Letters*, Vol. 21, No. 6, 2148–1252, 2022.

2. Tsai, J. F. and J. S. Row, "Reconfigurable square-ring microstrip antenna," *IEEE Transactions on Antennas and Propagation*, Vol. 61, No. 5, 2857–2860, 2013.

3. Kovitz, J. M., H. Rajagopalan, and Y. Rahmat-Samii, "Design and implementation of broadband MEMS RHCP/LHCP reconfigurable arrays using rotated E-shaped patch elements," *IEEE Transactions on Antennas and Propagation*, Vol. 63, No. 6, 2497–2507, 2015.

4. Zhang, Y. W., L. Shu, Z. Q. Yang, B. Q. Li, J. X. Cui, and J. L. Jiao, "A pattern- and frequency-reconfigurable antenna using liquid metal," *Microwave and Optical Technology Letters*, Vol. 63, 1499–1506, 2021.

5. Bai, X., S. Lv, and Y. J. Zhu, " A dual-polarized, direction diagram reconfigurable, liquid metal antenna," *Progress In Electromagnetics Research Letters*, Vol. 106, 57–66, 2022.

6. Song, L., W. Gao, C. Chui, and Y. Rahmat-Samii, "Wideband frequency reconfigurable patch antenna with switchable slots based on liquid metal and 3-D printed microfluidics," *IEEE Transactions on Antennas and Propagation*, Vol. 67, No. 5, 2886–2895, 2019.

7. Alqurashi, K., J. Kelly, Z. Wang, and et al., "Liquid metal bandwidth reconfigurable antenna," *IEEE Antennas and Wireless Propagation Letters*, Vol. 19, No. 1, 218–222, 2020.

8. Rodrigo, D., L. Jofre, and B. Cetiner, " Circular beam-steering reconfigurable antenna with liquid metal parasitics," *IEEE Transactions on Antennas and Propagation*, Vol. 60, No. 4, 1796–1802, 2012.

9. Chen, Z., H. Wong, and J. Kelly, "A polarization-reconfigurable glass dielectric resonator antenna using liquid metal," *IEEE Transactions on Antennas and Propagation*, Vol. 67, No. 5, 3427–3432, 2019.

10. Zhang, G. B., R. C. Gough, M. R. Moorefield, et al., "A liquid-metal polarization-pattern-reconfigurable dipole antenna," *IEEE Antennas and Wireless Propagation Letters*, Vol. 17, No. 1, 50–53, 2018.

11. Xu, C., Y. Wang, J. H. Wu, and Z. P. Wang, "Parasitic circular patch antenna with continuously tunable linear polarization using liquid metal alloy," *Microwave and Optical Technology Letters*, Vol. 3, 1–7, 2018.

12. Wang, C., J. C. Yeo, H. Chu, C. T. Lim, and Y. X. Guo, "Design of a reconfigurable patch antenna using the movement of liquid metal," *IEEE Antennas and Wireless Propagation Letters*, Vol. 17, No. 6, 974–977, 2018.

13. Liu, Y., Q. Wang, Y. T. Jia, and P. S. Zhu, "A frequency- and polarization-reconfigurable slot antenna using liquid metal," *IEEE Transactions on Antennas and Propagation*, Vol. 68, No. 11, 7630–7635, 2020.

14. Song, L. N., W. R. Gao, and Y. Rahmat-Samii, "3-D printed microfluidics channelizing liquid metal for multipolarization reconfigurable extended E-shaped patch antenna," *IEEE Transactions on Antennas and Propagation*, Vol. 68, No. 10, 6867–6878, 2020.

15. Ehrenspeck, H. W., "A new class of medium-size high-efficiency reflector antennas," *IEEE Transactions on Antennas and Propagation*, Vol. 22, No. 2, 329–332, 1974.